



# The Effects of Carbide Characteristics on the Performance of Tungsten Carbide-Based Composite Overlays, Deposited by Plasma-Transferred Arc Welding

G. Fisher, T. Wolfe, and K. Meszaros

(Submitted September 27, 2012; in revised form November 14, 2012)

**In Alberta, there are huge quantities of ore processed to remove bitumen from oil sands deposits. The scale of production generates very aggressive tribocorrosive conditions during the mining, extraction, and upgrading processes. It is common to apply tungsten carbide-based composite overlays to improve the reliability and extend service lives of equipment and components. The performance of the applied overlays is largely dependent on the selection of the carbide type and the wear environment. This paper will evaluate overlays containing macrocrystalline, angular eutectic, and spherical eutectic tungsten carbides and discuss the performance of the overlays with a focus on carbide properties and the interactions between the service conditions and the composite material. This discussion will demonstrate how effective selection of protective materials can improve the reliability of oil sands equipment.**

**Keywords** abrasion, overlay, PTAW, tungsten carbide

## 1. Introduction

The Athabasca oil sands deposits cover a region of 14,200 km<sup>2</sup> in the north east of Alberta, Canada. The proven reserves of recoverable oil are estimated at 171 billion barrels, making the reserve the third largest in the world, after Saudi Arabia and Venezuela (Ref 1). The oil sands are currently processed primarily by surface mining. Oil sands deposits are removed via truck and shovel operations and sized using crusher/conveyor systems. The processed sands are then mixed with water and other additives to form a slurry, which is piped using a hydrotransport system to an extraction plant for further processing (Ref 2). The oil sands are comprised of quartz sand, silt, clay, water, and bitumen (Ref 3). The bitumen content of the deposits tends to range from 1 to 18%, with levels of greater than 12% being considered a “rich deposit.” Quartz sands typically comprise between 80 and 95% of the total solids in the ore and are generally angular and less than 150 μm in size (Ref 4).

The extent of the mining and processing operations, with the associated high levels of wear and corrosion-induced damage, has led to high maintenance costs and significant production losses at the four commercial mine sites. In 2011, the operating costs at the four facilities

could be estimated at approximately \$5 billion (Ref 5). A major portion of this budget is due to wear damage to components and machinery (Ref 6).

The standard alloys used in mining and petrochemical applications do not have the wear and corrosion resistance necessary to withstand the aggressive processing conditions prevalent throughout the surface mining process. As such, there has been a wide adoption of wear- and corrosion-resistant materials to increase component reliability and longevity. By applying weld overlays, it is possible to retain the desired properties of the bulk material used to produce a component, while vastly improving the protective qualities of the surfaces in contact with the sand media. Two main types of overlays are employed: chromium carbide-based alloys and tungsten carbide-based metal matrix composites. Chromium carbide-based hardfacing alloys are essentially high chromium cast irons, which contain a distribution of acicular chromium carbides in an iron-based austenitic or martensitic matrix. Compared to other types of wear-resistant materials (e.g., polymeric liners and tungsten carbide-based overlays), chromium carbide-based overlays are relatively inexpensive. As such, they tend to be used for high volume applications, such as hydrotransport pipes (Ref 7).

Tungsten carbide-based metal matrix composite (MMC) overlays, deposited by plasma-transferred arc welding (PTAW), are currently the protective materials of choice for critical production applications. The composites typically comprise of either 60 or 65 w% tungsten carbide particles within a nickel-based matrix alloy (Ref 8). The carbides are either monocrystalline WC or a eutectic WC/W<sub>2</sub>C. The eutectic carbides are available as either angular or spherical particles, while WC is only produced as an angular powder (Ref 9).

G. Fisher, T. Wolfe, and K. Meszaros, Alberta Innovates—Technology Futures, Edmonton, AB, Canada. Contact e-mail: Gary.Fisher@albertainnovates.ca.

Abrasion is the most common form of wear in oil sands processing (Ref 10). Particle properties that affect abrasivity include hardness, angularity, population, and the size of an abrasive. With regard to sand size, it has been previously reported that the size of an abrasive has only a negligible effect on the wear rates of alloys when the particles are greater than 100  $\mu\text{m}$  (Ref 11). The effects of sand size on the abrasion resistance of tungsten carbide-based composite overlays have not been fully reported. The objective of this paper is to evaluate the effects of sand size on the abrasion resistance of three types of tungsten carbide-based MMC overlays, including an evaluation of how carbide properties affect the wear resistance of the composite. Preliminary work on a test method to characterize the fracture toughness of carbide powders will also be presented.

## 2. Materials

Three powder blends, detailed in Table 1, were employed for this assessment. The two commercial powders were produced by Sulzer Metco Inc. (Fort Saskatchewan, AB, Canada). The 6030M powder contains 60 wt.% monocrySTALLINE WC with 40 wt.% NiCrBSi (30 HRC) matrix alloy. The 6040 powder is a blend of 60 wt.% eutectic WC/W<sub>2</sub>C with 40 wt.% NiCrBSi (40 HRC). The nominal particle size range of both powders was 53-180  $\mu\text{m}$ . The third powder containing spherical carbides was a non-commercial blend, combining 60 wt.% spherical eutectic WC/W<sub>2</sub>C (size range 225-275  $\mu\text{m}$ ) with 40 wt.% NiCrBSi (40 HRC) matrix alloy. The spherical carbides were produced by Kennametal (Rogers, AR, USA), while the matrix alloy was supplied by Advanced Alloys (Deer Park, NY, USA).

The PTAW overlay deposition of the MMC powders was conducted using a Stellite Starweld 300 M constant current power source with a Stellite Excalibur PTAW torch. The thoriated-tungsten electrode was 4.8 mm in diameter, and the electrode tip angle was maintained between 10 and 20 °C. The electrode setback distance was set at 3.2 mm. The table was stationary and the torch was maneuvered by a Siemens Simatic OP7 controller interface and Millermatic Weld Oscillator. The ranges of parameters used to deposit the overlays are shown in Table 2.

## 3. Experimental Procedure

### 3.1 Microstructural Analysis

The coupons were sectioned from the welded deposits using a diamond-bonded wafering blade and were

metallurgically prepared in cross section using standard polishing procedures and consumables. Micrographs were taken and image analysis conducted using a Hirox KH-8700 digital microscope system. Scanning electron microscopy (SEM) was conducted using a Hitachi S-3000N SEM with a Quartz-1 EDS analyzer.

### 3.2 Wear Testing

Dry sand, rubber wheel (DSRW) abrasion testing was conducted according to a modified version of ASTM standard *G65-04 (2010)—Standard test method for measuring abrasion using sand/rubber wheel apparatus*. Due to the unavailability of the chlorobutyl rubber specified in the ASTM standard, a modified test procedure using a neoprene compound to line the test wheels was utilized. In the tests, four grades of sand with different size ranges were employed:

- 20/30 mesh (595-840  $\mu\text{m}$ ),
- 50/70 mesh (210-297  $\mu\text{m}$ ),
- 50/270 mesh (53-297  $\mu\text{m}$ ), and
- <325 mesh (<45  $\mu\text{m}$ ).

The first three sand types were obtained from the U.S Silica Company (Ottawa, USA), while the fourth grade of sand (<325 mesh) was sourced from SIL Industrial Minerals, (Edmonton, AB, Canada). SEM micrographs of the sands are shown in Fig. 1.

Procedure A (6000 revolution test) of the ASTM standard was used to evaluate abrasion resistance. Samples were ground to the required dimensions as specified in the ASTM standard. Two tests were conducted per specimen, the second test being performed directly on the wear scar produced by the first test. Due to the hard and soft dual-phase microstructure of the MMCs, the first test is used to condition the sample, exposing the primary carbide particles. This allows the second test to be conducted under more “steady-state” conditions.

**Table 2** Deposition parameters used to produce the overlays

Deposition parameter	Details
Amperage	120-140 A
Voltage	25-27 V
Stand-off distance	13 mm
Powder flow rate	25-30 g/min
Transverse width	17
Interpass temperature (°C)	180-200 °C

**Table 1** Details of the three composite powders

Powder ID	Carbide type	Alloy composition, wt.%				
		Ni	Cr	B	Si	C
6030M	Angular WC (53/180 $\mu\text{m}$ )	Bal	5.0-6.5	0.8-1.2	3.8-4.3	0.2-0.4
6040	Angular WC/W <sub>2</sub> C (53/180 $\mu\text{m}$ )	Bal	5.5-8.0	0.8-1.2	3.8-4.3	0.2-0.4
Sph-40	Spherical WC/W <sub>2</sub> C (225/275 $\mu\text{m}$ )	Bal	7.63	1.66	3.62	0.27

## 4. Results and Discussion

### 4.1 Overlay Microstructures

The three overlays contained relatively homogeneous distributions of primary tungsten carbide particles in the nickel-based matrix alloys. As an example, Fig. 2 shows a micrograph of the 6030M overlay. The carbides are well distributed, and there is little or no evidence of primary carbide dissolution. The overlays containing the angular and spherical eutectic carbides were found to have been subject to a degree of carbide dissolution (Fig. 3). The heat produced during the deposition of MMC powders can promote the dissolution of the primary tungsten carbide powders (Ref 12). Eutectic WC/W<sub>2</sub>C can decompose into W and WC below 1250 °C (Ref 13). The W<sub>2</sub>C-phase in the eutectic dissolves and reprecipitates as a (Cr, Ni)-containing polymorphs of W<sub>2</sub>C ( $\beta$ - and  $\alpha$ -) or  $\eta$ -carbides (Ref 14). The degree of dissolution is affected by the deposition parameters; higher amperage or voltage increases the heat in the weld pool, promoting the degradation of the carbides (Ref 15). Monocrystalline WC is thermally stable up to 2757-2777 °C (Ref 16), and so is far less likely to decompose and react with the metal alloy. As such, WC-based MMC overlays are more widely used in the oil sands industry as the stability of WC allows for a wider window of production parameters and improved consistency (Ref 17).

### 4.2 Abrasion Resistance of Tungsten Carbide-MMC Overlays

Overlays deposited using the 6030M powder underwent abrasion testing using the four sand sizes. The results of the testing, expressed as mass loss, are shown in Fig. 4. The fine sand [ $<325$  mesh ( $<45 \mu\text{m}$ )] had preferentially removed the matrix alloy (Fig. 5a), with the sand being channeled between the WC particles. The level of wear-induced damage to the carbide particles appeared to be very low; the particles displayed no appreciable levels of chipping or fracturing.

The worn surfaces on the samples abraded by the 50/270 mesh (53-297  $\mu\text{m}$ ) and 50/70 mesh (210-297  $\mu\text{m}$ ) sands were very similar. This indicates that the wear mechanisms were comparable for both size ranges of sand abrasive, with the preferential removal of the matrix alloy leaving the primary carbides proud to the surface (Fig. 5b). The wear mechanism displayed by the MMC is related both to the size of the abrasive and the mean free path ( $\lambda$ ) of the WC particles in the composite. The  $\lambda$  of the WC in the 6030M overlay was measured using an intercept method, ten lines per field of view at a magnification of 50 $\times$ . The average  $\lambda$  was measured as 43  $\mu\text{m}$ . The average size of each of the grades of sand was larger than the  $\lambda$  of the carbides. It is assumed that the angularity of the sand particles allowed for the points of contact between the abrasives and the MMC to

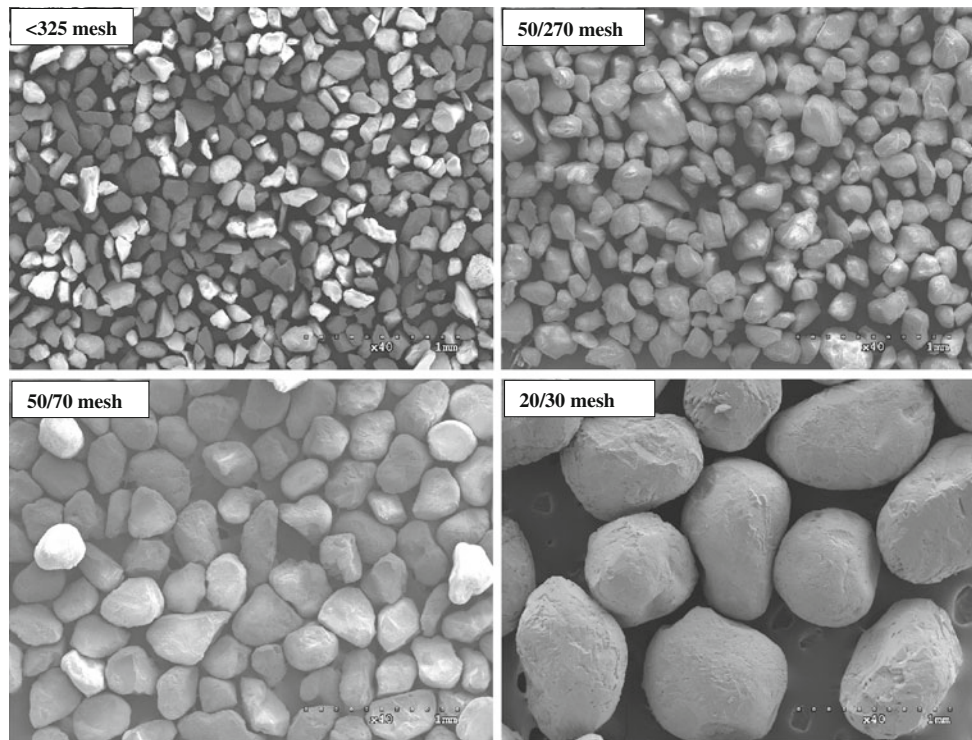


**Fig. 1** SEM micrographs of the three test sands

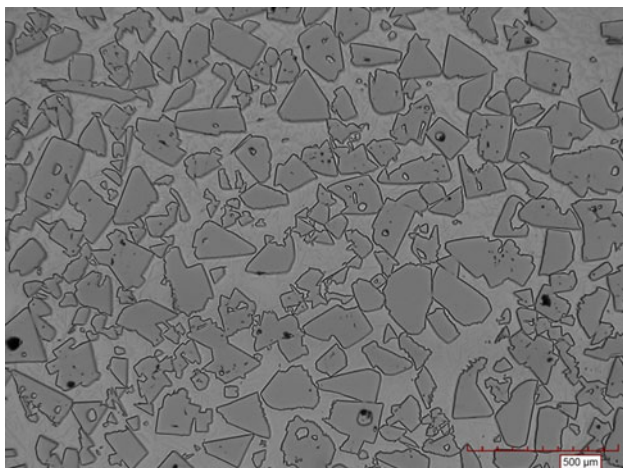


**Fig. 2** Micrograph of the 6030M overlay, showing the distribution of WC particles in the Ni-alloy matrix. Magnification 140×

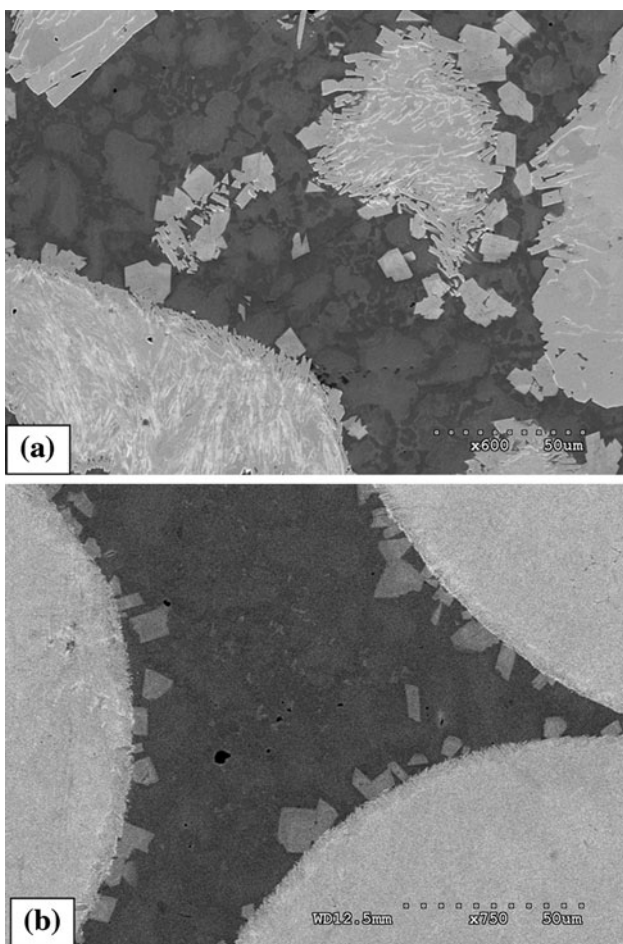


**Fig. 3** SEM micrographs showing the dissolution and secondary carbide formation in the two eutectic-based MMC overlays. (a) 6040M, magnification 600×, (b) Sph-40, magnification 750×

be less than the average  $\lambda$ . This allowed for the passage of the sand to be preferentially between the WC particles.

Evidence of damage to the WC particles was more apparent, with the carbides being subjected to chipping and crazing. The increased fracturing of the WC was probably related to the larger sand particle size producing a higher relative loading for each abrasive contacting the surface.

The effect of particle size on the rate of material removal was even more palpable for the overlay sample abraded with the 20/30 mesh (595–840  $\mu\text{m}$ ) sand. The large sand particles had caused extensive damage to both the matrix and carbide phases (Fig. 5c). The Ni-based matrix alloy displayed evidence of being removed by a process of extrusion and cutting, while the WC particles were subject to multiple chipping and cleavage-type fractures. Unlike the other sands, the second wear test using the 20/30 mesh (595–840  $\mu\text{m}$ ) sand produced a higher level of material wastage due to the extensive fracturing and loss of the primary carbides. The higher levels of damage to the MMC can be accounted for by the higher stress exerted by the larger abrasive particles. The abrasion testing was conducted using a fixed flow rate of 340 g/min at a set applied load of 130 N. By increasing the size of the abrasive, the applied force is distributed through a lower number of particles. As such, the applied force per abrasive particle increases (Ref 18). This accounts for the increase in carbide fracturing, and the resultant higher mass losses, when abraded with the larger sands.

To determine the effects of primary carbide type on abrasion resistance, samples of the overlays produced using the eutectic carbide powders underwent abrasion testing using the 50/70 mesh (210–297  $\mu\text{m}$ ) and 20/30 mesh (595–840  $\mu\text{m}$ ) sands. These results are compared to the 6030M overlay, as shown in Fig. 6. When abraded with the 50/70 mesh (210–297  $\mu\text{m}$ ) sand, the 6040 overlay produced slightly higher levels of material loss, compared to the 6030M overlay. This was probably due to a combination of slightly more chipping to the WC/W<sub>2</sub>C carbides and the increased removal of the matrix phase that may have become slightly embrittled due to the presence of the secondary carbide precipitates.

Abrasion with the coarse 20/30 mesh (595–840  $\mu\text{m}$ ) sand produced a higher level of material loss than the 50/70 mesh (210–297  $\mu\text{m}$ ). The MMCs were subject to a similar wear mechanism, with extensive fracturing of the primary carbides and deformation of the matrix (Fig. 7); however, the rate of material loss was lower for the eutectic carbides (6040 and Sph-40) than for the 6030M overlay.

When abraded using the 50/70 mesh (210–297  $\mu\text{m}$ ), the Sph-40 MMC produced similar levels of wear as the 6030M overlay. As before, the sand particles had been channeled between the carbides, removing the matrix alloy. The spherical carbides were left proud to the surface and displayed no significant levels of chipping or fracturing (Fig. 8a). When abraded with the larger 20/30 mesh (595–840  $\mu\text{m}$ ) sand, the MMC recorded only slightly higher levels of material loss. The levels of carbide fracturing appeared to be notably lower than for the angular carbide-containing composites (Fig. 8b). The spherical carbides were the most resistant to abrasive wear.

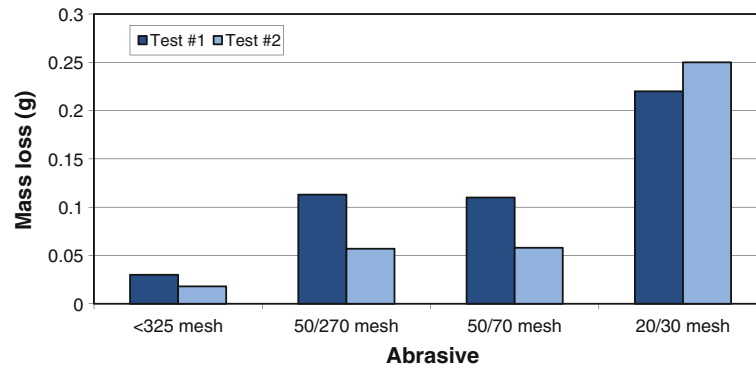


**Fig. 4** Chart showing abrasion testing results for the 6030M overlay, abraded with the four sizes of test sand

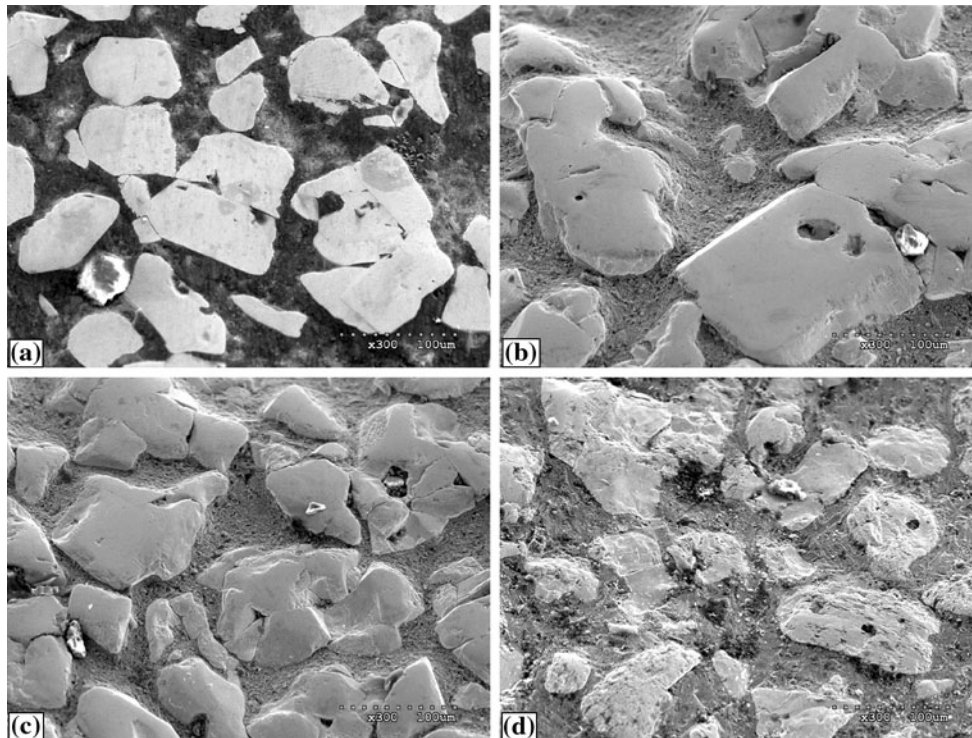


**Fig. 5** SEM micrograph showing the surface of a 6030M overlay abraded with the (a) <325 mesh, (b) 50/270 mesh, (c) 50/70 mesh, or (d) 20/30 mesh test sands. Magnification 300×

The difference in the performance of the MMCs may be linked to the fracture toughness of the primary tungsten carbide phases. This can be partially explained by the crystallography of the carbides. Monocrystalline tungsten carbide has a hexagonal crystal structure with anisotropic properties (Ref 19), whereby the crystal orientations containing the closest packed tungsten atoms have a higher hardness. The measured hardness for a close-packed orientation such as {0001} is 2100 Hv, as compared to the {1100} orientation, with a hardness of 1080 Hv. The lower hardness crystal orientations are also reported to be more susceptible to cracking (Ref 20).

Microhardness testing was conducted on a sample of WC produced by Sulzer Metco. A 10-g sample of

53/180  $\mu\text{m}$  powder was mounted in a cold setting epoxy and metallographically prepared in cross section. Vickers microhardness testing was conducted, using a 300-g load and a 15-s duration. Thirty indents were performed. The carbide was found to have an average hardness of 1495 Hv, with a range of hardness values from 1187 to 2017 Hv. As such, the measured hardness of the carbide was within the ranges recorded by Takahashi et al (Ref 19).

It seems probable that the high level of material removal recorded for the 6030-M overlay is related to the anisotropic properties of the WC, with the fracture toughness of the material being dependent on the orientation of the particle. The angular and spherical eutectic WC/W<sub>2</sub>C particles were not subject to this phenomenon.

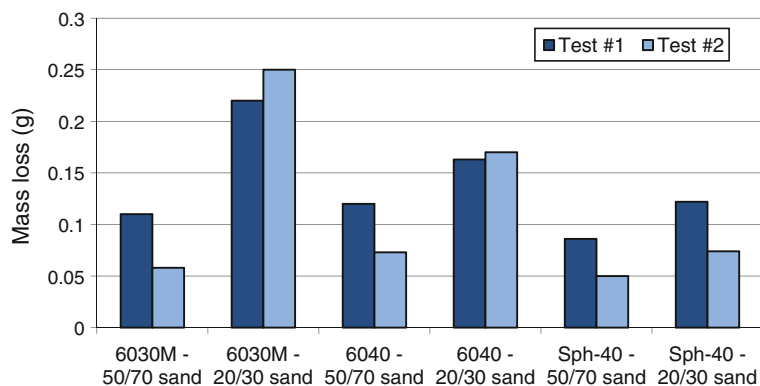


**Fig. 6** Chart showing the abrasion test results achieved by the three types of MMC overlay, abraded with either 50/70 or 20/30 mesh sands



**Fig. 7** SEM micrograph showing the surface of the 6040 overlay, after abrasion by the 20/30 mesh sand. Magnification 1000×

The relatively higher fracture toughness of the carbides produced lower levels of mass loss when abraded with the coarse sand. These results are in line with the findings of Ottonello (Ref 21), which recommend the use of spherical carbides for high load and impact applications.

For applications that will experience high stress abrasion or impact (for example, ground engaging tools or sizing equipment), it may be preferable to utilize a carbide that displays higher fracture toughness. At present, there is no known quantitative method to effectively measure the fracture toughness of tungsten carbide powders. The diamond abrasives industry has developed test procedures to quantitatively measure the friability of powders (Ref 22-24). This procedure is currently being modified to allow for the testing of tungsten carbide powders.

The friability test for the tungsten carbide powders, sized to 120-180  $\mu\text{m}$ , is tested in 10-g charges. The sample of carbide powder is placed in a metal container with eight carbide balls (diameter 1.6 cm). The container is then tumbled in a powder mixer for 10 min at a frequency of 67 rpm. The mass of the carbide balls and the charge powder are measured individually before and after the

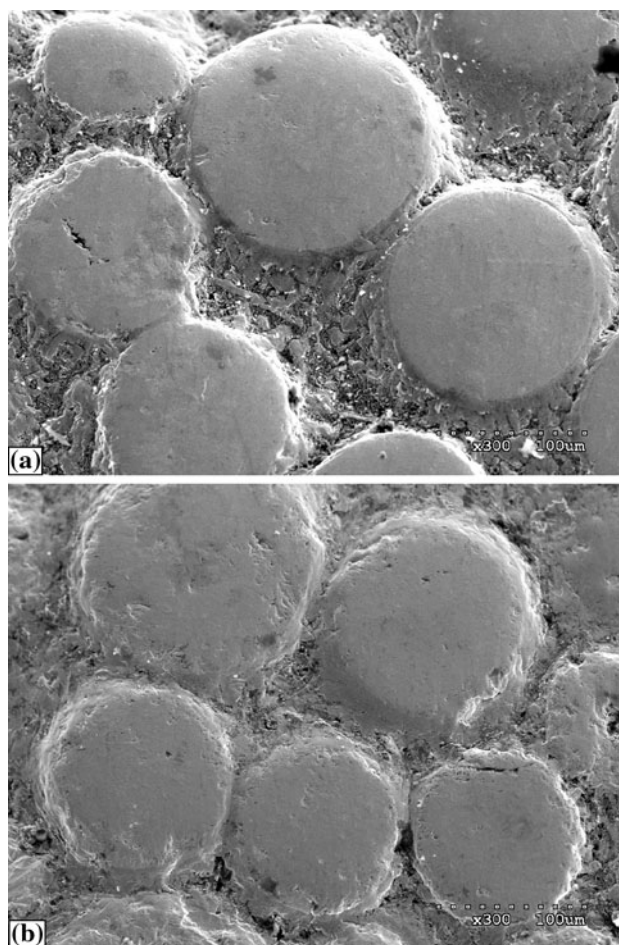


**Fig. 8** SEM micrograph showing the surface of the Sph-40 overlay, after abrasion by either (a) 50/70 mesh sand or (b) 20/30 mesh sand. Magnification 300×

tumbling procedure. The crushed powders are then analyzed to measure their particle size distribution. Three samples of each of the tungsten carbide powders (WC, angular WC/W<sub>2</sub>C, and spherical WC/W<sub>2</sub>C) have been tested. The results, presented as averages, are shown in

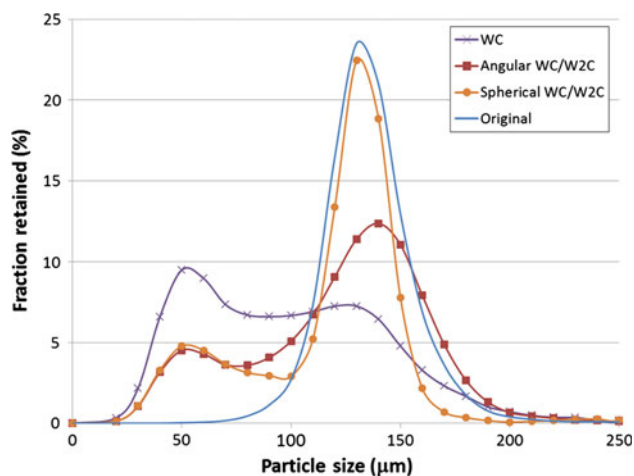


Fig. 9 Friability results

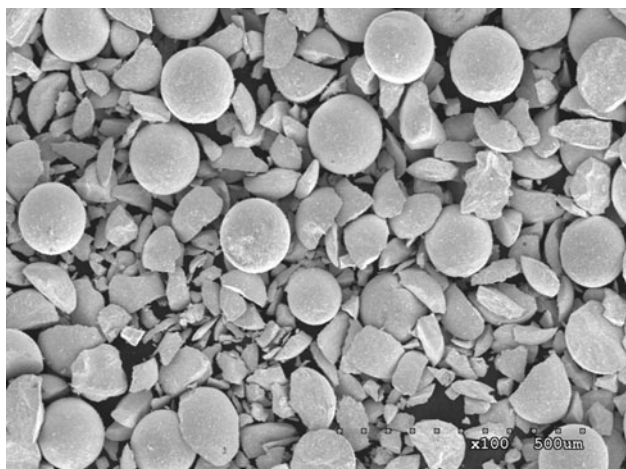


Fig. 10 SEM of spherical carbide powder, after friability testing, showing the degree of carbide fracturing. Magnification 100×

Fig. 9. To demonstrate the level of fracturing, Fig. 10 shows the spherical carbide powder after friability testing.

The WC powder was subject to far higher fracturing, producing a higher number of smaller carbide particles in the range of 50-75 µm and a significant reduction from the original size distribution. Both eutectic powders recorded lower levels of fracturing. The spherical WC/W<sub>2</sub>C carbides experience very little difference from the original distribution: The larger sized particles were more susceptible to cracking. The eutectic (angular and spherical) carbides are more resistant to fracturing than the monocrystalline carbides. It can be inferred that the fracture toughness of the eutectic powders is likely to be higher than the monocrystalline WC, which is supported by the abrasion testing results.

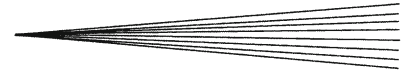
This new test method has shown that it is possible to quantifiably distinguish between tungsten carbide powders with varying fracture toughness. This technique could be further developed as a practical tool to enable the improved selection of tungsten carbide-based materials for specific applications.

## 5. Conclusions

1. Eutectic (WC/W<sub>2</sub>C) primary carbides are more susceptible to dissolution due to heat input upon deposition. The levels of secondary carbide formation for the monocrystalline (WC)-containing 6030M overlay were significantly lower.
2. Abrasion by sands sized less than 350 µm (50 mesh) preferentially removed the matrix alloy in the MMC.
3. The abrasion rates recorded by the WC-MMC were related to the size of the abrasive and the associated applied load. Increases in these two factors produced higher levels of mass loss due to primary carbide fracturing.
4. The fracture toughness of the tungsten carbide is a key factor in determining the abrasion resistance of the MMC. The eutectic carbides displayed higher resistance to fracturing than the WC.
5. A test method has been developed that can quantify the fracture toughness of tungsten carbide powders. This procedure could be developed as a technique to aid the selection of MMCs for specific applications in mining facilities.

## References

1. <http://oilsands.alberta.ca/resource.html>
2. M. Anderson, S. Chiovelli, and S. Hoskins, *Improved Reliability and Productivity at Syncrude Canada Ltd. Through Materials Research: Past, Present and Future*, CIM Bulletin, October 2004, pp. 1-6
3. J. Flores and A. Neville, Materials Selection in the Oil Sands Industry Based on Materials Degradation Mechanisms, *Explor. Prod.*, 2009, 7(1), p 42-45
4. P. Bayliss and A. Levinson, Mineralogical Review of Alberta Oil Sands Deposits (Lower Cretaceous, Manneville Group), *Bull. Can. Petrol. Geol.*, 1974, 24(2), p 211-214
5. D. Harper, M. Gill, K Hart, and M. Anderson, *Plasma Transferred Arc Overlays Reduce Operating Costs in Oil Sands Processing*, International Thermal Spray, 2002, Essen, Germany
6. G. Fisher, *Protective Coatings and Overlay: Development of Wear and Corrosion-Resistant Coatings in Oil Sands Mining*, Canadian Chemical News, June 2006, pp. 12-13
7. G. Fisher, T. Wolfe, M. Yarmuch, A. Gerlich, and P. Mendez, The Use of Protective Weld Overlays in Oil Sands Mining, *Can. Weld. Assoc. J.* Summer 2011, p 28-40
8. J.F. Flores, A. Neville, N. Kapur, and A. Gnanavelu, An Experimental Study of the Erosion-Corrosion Behaviour of Plasma Transferred Arc MMCs, *Wear*, 2009, 267, p 213-222
9. Ch. Just, S. Ilo, and E. Badisch, Influence of Processing Conditions on the Carbide/Matrix Interface in Sintered Composite Layers, *Surf. Coat. Technol.*, 2010, 205, p 35-42
10. R. Llewellyn, Materials for Controlling Wear in Surface Mining, *CIM Bulletin*, 1996, 89(1002), p 76-82
11. E. Rabinowicz, A Study of Abrasive Wear Under Three-Body Conditions, *Wear*, 1961, 4, p 345-355
12. Ch. Just, E. Badisch, and J. Wosik, Influence of Welding Current on Carbide/Matrix Interface Properties in MMCs, *J. Mater. Process. Technol.*, 2010, 210, p 408-414
13. H. Pierson, *Handbook of Refractory Carbides and Nitrides*, William Hill Publishing, Norwich, 1996
14. L. Choi, T. Wolfe, M. Yarmuch, and A. Gerlich, Effect of Welding Parameters on Tungsten Carbide—Metal Matrix Composite (WC-MMC) Produced by GMAW, CWA Conference, August 2010



15. C. Katsich and E. Badisch, Effect of Carbide Degradation in a Ni-Based Hardfacing Under Abrasive and Combined Impact/Abrasive Conditions, *Surf. Coat. Technol.*, 2011, **206**, p 1062-1068
16. A.S. Kurlov and A.I. Gusev, Tungsten Carbides and W-C Phase Diagram, *Inorg. Mater.*, 2006, **42**, p 156-163
17. M. Anderson, S. Chiovelli, and R. Llewlyn, The Use of Tungsten Carbide Materials for Oilsand Wear Applications, *Thermal Spray 2003*, C. Moreau and B. Marple, Eds., ASM International, 2003, p 509-518
18. I.M. Hutchings, Tribological Properties of Metal Matrix Composites, *Mater. Sci. Technol.*, 1994, **10**, p 513-517
19. T. Takahashi and E.J. Freise, Determination of the Slip Systems in Single Crystals of Tungsten Monocarbide, *Philos. Mag.*, 1964, **12**, p 1-8
20. B. Nayak, Enhancement in the Microhardness of Arc Plasma Melted Tungsten Carbide, *J. Mater. Sci.*, 2003, **38**, p 2717-2721
21. G.B. Ottonello, Tungsten Carbides and Welding, *Weld. Int.*, 2007, **21**(8), p 569-583
22. D.E. Cadwell and E.H. Duwell, Evaluating Resistance of Abrasive Grits to Comminution, *Ceram. Bull.*, 1960, **39**(11), p 663-667
23. N.G. Belling and H.B. Dyer, The Friatester—10 years later, *Ind. Diamond Rev.*, 1974, **8**, p 285-291
24. Y. Zhou, T. Takahashi, D.J. Quesnel, and P.D. Funkenbush, Friability and Crushing Strength of Micrometer Size Diamond Abrasives Used in Microgrinding of Optical Glass, *Metall. Mater. Trans. A*, 1996, **27A**, p 1047-1053